The 56th International October Conference on Mining and Metallurgy
22-25 October 2025, Bor Lake, Bor, Serbia
www.ioc.tfbor.bg.ac.rs

DOI: 10.5937/IOC25526M
Original scientific paper

CHANGES IN HARDESS AND MICROSTRUCTURE DURING ISOTHERMAL AGING OF NICKEL-ALUMINUM BRONZE

Ivana Markovic[1a], Uroš Stamenković[1b], Dragan Manasijević[1c], Ljubiša Balanović[1d]

[1] University of Belgrade - Technical Faculty Bor, V.J. 12, 19210 Bor, Serbia
[1a] imarkovic@tfbor.bg.ac.rs, 0000-0003-4431-9921
[1b] ustamenkovic@tfbor.bg.ac.rs, 0000-0002-7579-2159
[1c] dmanasijevic@tfbor.bg.ac.rs, 0000-0002-7828-8994
[1a] ljbalanovic@tfbor.bg.ac.rs, 0000-0002-3551-6731

Abstract
In this paper, the properties and microstructural changes in Cu-Al-Ni-Fe bronze were studied during isothermal aging. The alloy was annealed at 900 °C for 2 hours following the casting process and quenched rapidly in cold water. Isothermal aging was then carried out up to 10 h at 350 °C, 400 °C, and 450 °C. During isothermal aging, hardness was tested and microstructure was examined using the scanning electron microscope. Isothermal aging at all selected temperatures contributed to a significant increase in hardness values. The alloy aged at 400 °C for 1 h achieved the highest relative hardness increase of 35 %, compared to the quenched state.

***Keywords**: nickel-aluminum bronze, isothermal aging, microstructure, hardness*

1. INTRODUCTION

Nickel-aluminum bronzes (NABs) are copper-based alloys containing 8–13% aluminum and 3–6% nickel, often with small amounts of iron, manganese, and other elements added to increase strength and corrosion resistance. NABs are highly valued in marine and industrial applications for their excellent combination of strength, toughness, and corrosion- and wear-resistance [1-4].

Microstructure of NABs is complex and has a significant influence on their mechanical and corrosion-resistant properties. Copper-rich α-phase is the dominant phase, which has a face-centered cubic crystal structure. The α-phase forms the alloy matrix and is relatively soft and ductile. During solidification and subsequent heat treatments, several intermetallic phases known as κ phases precipitate. These κ phases have a high concentration of aluminum, nickel, and iron and occur as small particles that harden the alloy by preventing dislocation movement, thereby improving strength and hardness. Examples of common κ phases include κ_I, κ_{II}, κ_{III}, and κ_{IV}, which differ in composition and morphology. The particle size, morphology, and distribution of these κ phases are highly susceptible to cooling rates and heat treatment conditions. Controlled precipitation of κ phases under proper conditions increases mechanical properties [1, 4-9].

Heat treatment constitutes a critical phase in achieving the maximum properties of the NABs. The alloys are typically solid solution-annealed and quenched rapidly to preserve a supersaturated solid solution. Intermediate-temperature aging treatments subsequently cause precipitation of κ phases. Aging enables precipitates of fine κ phase to develop in a homogeneous distribution within the α matrix. The precipitates increase hardness and strength through a resistance to dislocation flow. Changing the microstructure is possible through control over the heat treatment parameters. The combination of α-phase matrix and highly dispersed κ phases provides optimal wear resistance, toughness, and endurance to mechanical stresses [1, 5, 9].

A low nickel/iron CuAl9Ni2.6Fe3.3 is between the binary and multicomponent alloys in microstructure and mechanical properties. It shows a good combination of ductility with strength and hardness [10, 11]. But their mechanical properties are lower compared to standard NABs with higher Fe and Ni content. These properties can be improved by heat treatment, which was studied in this paper.

2. EXPERIMENTAL

After weighing the required quantities of copper and alloying elements (aluminum, nickel, and iron), the materials were melted in a flame-fired furnace. The molten alloy was then cast into a mold made up of a mixture of sand and clay. The obtained ingot, with a composition of CuAl9Ni2.6Fe3.3 (in wt.%), was cut using the "Mesotom - Struers" machine on samples for subsequent heat treatment processes. For solution treatment, samples were annealed at 900 °C for 2 h in the hydrogen-reducing atmosphere using a "T 40/600" tube furnace. The specimens were quenched instantly in cold water so that they would have a supersaturated solid solution. Quenched samples were aged in a furnace "Heraeus K 1150/2". Isothermal aging was conducted at 350 °C, 400 °C, and 450 °C, for a period of up to 10 h. In all the stages of heat treatment processes, hardness was tested and microstructure was studied. Hardness was determined using "VEB Leipzig" Vickers hardness tester with an applied load of 15 kg. Microstructural observation was performed by scanning electron microscopy (SEM) on a "Tescan Vega 3LMU" system.

3. RESULTS AND DISCUSSION

In the as-cast condition, the CuAl9Ni2.6Fe3.3 alloy demonstrated a hardness of approximately 150 HV_{15}. After solution treatment at 900 °C followed by rapid quenching, the hardness increased to 176 HV_{15}, indicating the formation of a supersaturated solid solution. The evolution of hardness during isothermal aging at 350 °C, 400 °C, and 450 °C is shown in Fig. 1.

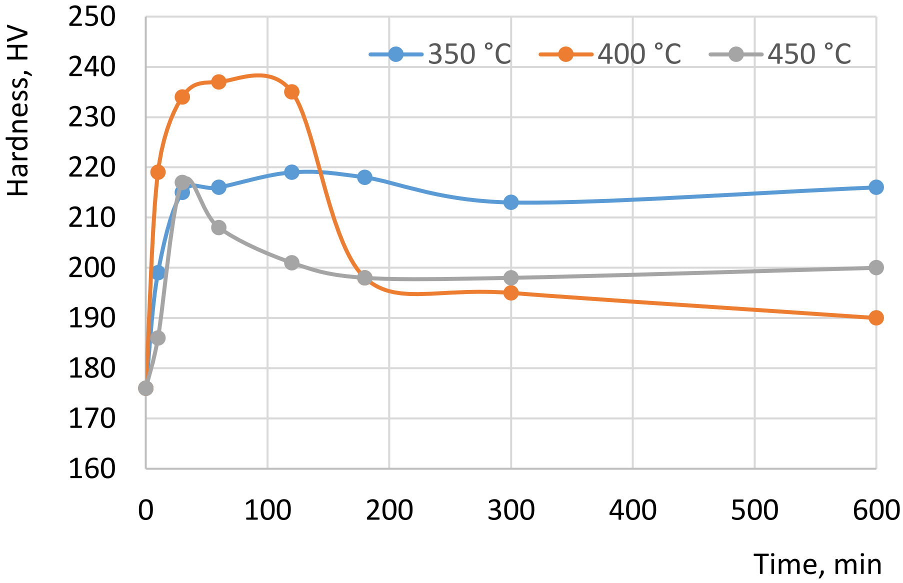

Figure 1. Hardness evolution during isothermal aging at 350 °C, 400 °C, and 450 °C after quenching from 900 °C

Aging at 350 °C led to a gradual increase in hardness with increasing aging duration. The maximum hardness of 219 HV_{15} was recorded after 2 h of aging, representing a significant enhancement compared to the quenched state. Further prolongation of aging up to 10 h did not result in a notable decrease, suggesting the alloy remained within the effective precipitation strengthening range.

The most substantial increase in hardness was observed at 400 °C, where a peak value of 237 HV_{15} was achieved after 1 h of aging. This corresponds to an absolute increase of 61 HV_{15}, or a relative improvement of approximately 35 % compared to the quenched condition. However, aging durations beyond 2 h resulted in a significant drop in hardness.

At the highest aging temperature of 450 °C, the alloy also exhibited an increase in hardness, reaching a maximum of 217 HV_{15} after only 30 min. However, the overall hardening response at this temperature was less pronounced. Prolonged aging beyond this point led to a decrease in hardness, indicating that the kinetics of overaging were accelerated at this temperature.

It is evident that with increasing aging temperature, the time required to reach peak hardness decreases. The highest overall hardness values were observed at the intermediate temperature of 400 °C, particularly in the aging range of 30 min to 2 h.

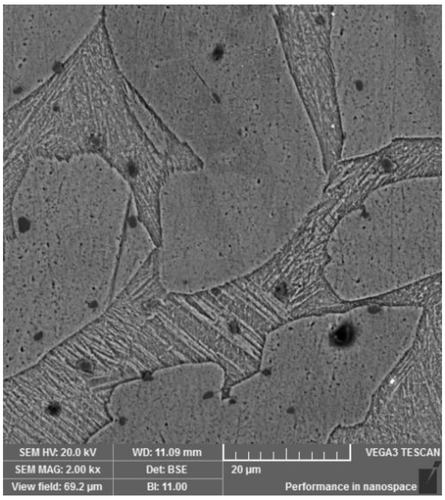

a)

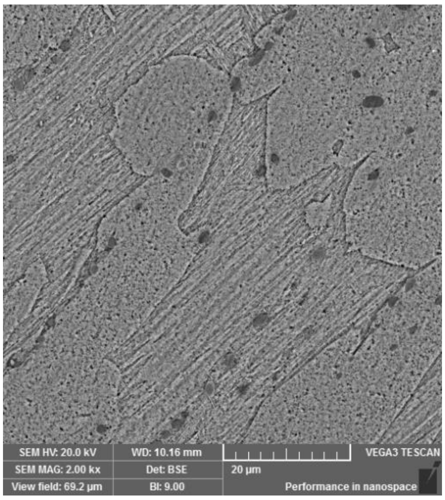

b)

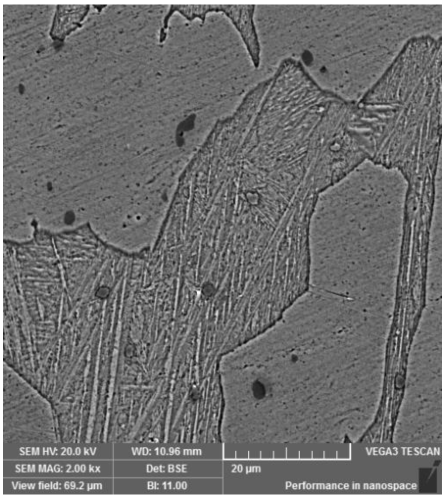

c)

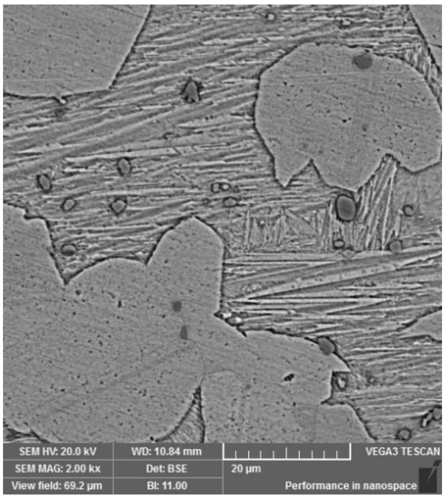

d)

Figure 2. Microstructure of CuAl9Ni2.6Fe3.3 alloy after (a) quenching from 900 °C and (b) aging at 350 °C; (c) aging at 400 °C; (d) aging at 450 °C

Fig. 2a shows the microstructure of the CuAl9Ni2.6Fe3.3 alloy after quenching at 900 °C. A α phase, a needle-like β' phase, as well as precipitates of the ƙ phases are observed. By quenching, the high-temperature β phase transformed into β' martensite. Eutectoid with the κ_{III} phase is not observed, because the κ_{III} phase dissolved at 800 ºC, and at 850 ºC the fine precipitates of the κ_{IV} phase also dissolved in the α solid solution [6]. Thus, α and β' phases and large spherical precipitates of κ_{I} and κ_{II} phases are presented in the microstructure.

Similarly, the microstructures of aged alloy (Fig. 2b-d) show the α phase and needles of β' martensite with spherical κ phases. Based on data from the literature, β' martensite does not transform into the α phase until above 550 °C [8,9]. Aging up to 450 °C of previously quenched samples from 900 °C did not cause significant microscopically visible changes in the size and shape of the main phases under the magnification of 2000x. The κ phases that precipitated during aging are finer (nano size) [12,13] than the precipitates formed during casting, so they are not distinguishable in the microstructure at this magnification.

4. CONCLUSION

After quenching, there was a slight increase in the hardness of the CuAl9Ni2.6Fe3.3 alloy compared to the as-cast state. Aging at all selected temperatures contributed to a significant increase in hardness values. The alloy aged at 400 °C for 1 h achieved the highest hardness values of 237 HV_{15}. With an increase in the aging temperature, there is a decrease in the aging time at which the maximum increase in hardness occurs. After aging at selected temperatures, α solid solution, β' martensite and ƙ phases are still observed in the microstructure, as in the microstructure of the quenched alloy.

ACKNOWLEDGEMENT

The research presented in this paper was done with the financial support of the Ministry of Science, Technological Development and Innovations of the Republic of Serbia, with the funding of the scientific research work at the University of Belgrade, Technical Faculty in Bor, according to the contract with number 451-03-137/2025-03/ 200131.

REFERENCES

[1] G. Lin, H. Wang, Y. Wei, Z. Zhang, K. Zhou, J. Mater. Res., 31 (2016) 3832–3840.
[2] F.A. Anene, V.U. Nwoke, S.M.O. Obiorah, Int. J. Multidiscip. Res. Dev., 2 (6) (2015) 338-341.
[3] K.K. Alanemea, U. J. Anaelea, A. E.Okotetea, Sci. Afr., 12 (2021) e00760.
[4] R. Chen, Z. Liang, W. Zhang, D. Zhang, Z. Luo, Y. Li, Trans. Nonferrous Met. Soc. China, 17 (6) (2007) 1254-1258.
[5] Y. Lv, L. Wang, Y. Han, X. Xu, W. Lu, Mater. Sci. Eng. A., 643 (2015) 17–24.
[6] P. Sláma, J. Dlouhý, M. Kövér, Materials and Technology, 48 (2014) 599–604.
[7] B.P. Pisarek, Arch. Foundry Eng., 11 (3) (2011) 187-194.
[8] M. Moradlou, N. Arab, R. Emadi, M. Meratian, J. Am. Sci., 7 (7) (2011) 717-722.
[9] Y. Lv, M. Hu, L. Wang, X. Xu, Y. Han, W. Lu, J. Mater. Res. 30 (20) (2015) 3041–3048.
[10] C.H. Meigh, Cast and wrought aluminium bronzes properties, processes and structure. McLean: Copper Development Association, 2008.
[11] H. Jiang, X. Zhang, R. Yang, Mater. Today Commun., 38 (2024)108152.
[12] Marković, M. Banković, D. Manasijević, Lj. Balanović, J. Petrović, Mater. Sci. Technol., 2025, doi: 10.1177/02670836241310747
[13] J.M. Da Silva, B.C.E.S. Kurelo, W.R. De Oliveira, A.G.M. Pukasiewicz, G.B. de Souza, S.F. Brunatto, Surf. Topogr.: Metrol. Prop., 10 (2022) 024007.